Performance of a VHF Ocean Surface Radar in the Surf Zone.

M.L. Heron and A. Prytz

Marine Geophysical Laboratory
James Cook University, Townsville, Australia 4811.
Mal.heron@jcu.edu.au

Abstract – **In the high VHF band (152.2 MHz) the Bragg scattering waves on the sea surface have wavelengths of about 1 m. The radar Doppler spectrum of echoes can be heavily modulated by swell in open water, and in the surf zone the effect is enhanced. Under these conditions the Bragg first-order lines are broadened This paper reports on a study to evaluate the integrity of the surface current maps produced by the VHF coastal ocean surface radar within the surf zone. Comparisons are made with radar data under calm conditions, and with currents measured with an acoustic current profiler mounted on the bottom. The radar current measurements are slightly more noisy under rough conditions, but it is clear that this technology has potential to monitor rip currents and coastal vortices in the surf zone when conventional techniques become strained.**

1. INTRODUCTION

The VHF coastal ocean surface radar (COSRAD), operating at 152.2 MHz, can make independent measurements of surface current on a grid spacing of the order of 100m. This makes it a useful and unique instrument to monitor currents in nearshore zones around channel openings and coastal engineering works. The VHF COSRAD system developed by James Cook University has been deployed to assist in planning sewerage outfalls and sediment transport management at various locations. Questions about the effect of breaking surf arise naturally when applications are considered for monitoring rip currents and other return currents on energetic ocean beaches.

The data used here were taken at Boambee Beach on the north coast of New South Wales on the east coast of Australia (30° 18' 50.8" S, 153° 08' 36.5" E) in order to investigate recirculation behind a headland during the planning of a new sewerage outfall by the Coffs Harbour City Council.

The radar data were evaluated against a NORTEK Acoustic Doppler Current Profiler (ADCP) which was bottom-mounted in a frame in 14 m deep water. The ADCP site was in the white water surf zone under rough conditions, and in blue water under calm conditions. The operating range of the VHF COSRAD system is about 1.5 km, so the surface current maps always extended beyond the surf, even in rough conditions.

2. THE VHF COSRAD SYSTEM

The VHF COSRAD system is an ocean surface backscatter radar operating at 152.2 MHz. It is used to measure surface currents (speed and direction) and has the potential to be used to infer sea state and wind direction. The maximum operating range for the radar is about 1.5 km, and the spatial resolution (grid scale) is about 100 m. These spatial specifications are ideally suited to the northern end of Boambee Beach where there is a peninsula, Corambirra Point, which protrudes about 1 km from the beach. The VHF COSRAD system requires two radar sites operating simultaneously to produce 2D surface current maps. In this deployment, one station was located on Corambirra Point, and the other was installed on the dunes at the back of Boambee Beach. The configuration of the deployments is shown in Figure 1.

Each VHF COSRAD station uses a beam-forming antenna to produce an effective 3 db beam width of 18

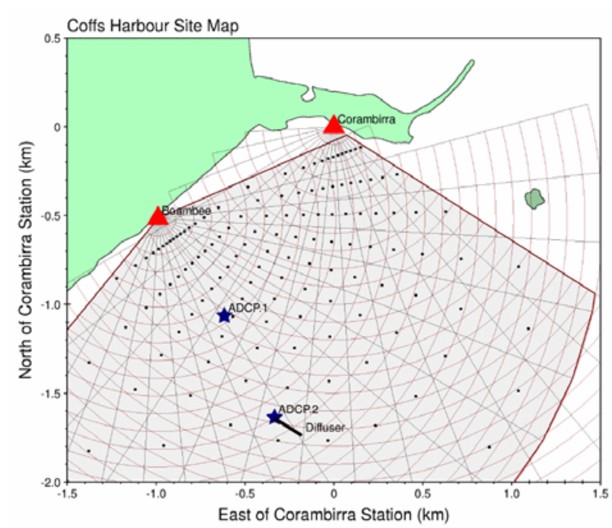

Fig 1. The site configuration at Boambee Beach. The VHF COSRAD stations are marked with triangles and ADCP1 is the *in situ* current measurement which was simultaneous with the radar data. ADCP2 was used at a later date at the site of the proposed diffuser oulet. The axes are referenced to the Corambirra Point station at 30° 18' 50.8" S, 153° 08' 36.5" E.

degrees. This beam is steered mechanically on a rotating boom by a stepper motor under the control of the station computer. The beam was set in one direction for 176 seconds to collect information from all range cells in that direction, and was then moved to the next position. The dwell times and steps were configured so that a new map of surface currents is produced every hour. The truly independent sampling grid is shown in Fig. 1 by dots at the beam intersection points. The sampled pixels are defined by the beam width and the time-gating on the radar A-scan. The pixels are irregularly shaped but have a scale size of about 100m. In practice, a finer grid can be used wherein the data points are only quasi-independent. This approach is commonly used by direction-finding ocean surface radar systems and lends itself well to spatial smoothing.

The backscatter of VHF electromagnetic waves from the sea surface is by a Bragg reflection where the radio wave with wavelength λ interacts with the surface gravity wave with wavelength λ/2 travelling in the same direction (there is a ± ambiguity here) (Crombie, 1955). The Bragg scatter dominates the return echoes to the radar as shown in Fig. 2, where the two dominant peaks in the echo spectrum correspond to the surface gravity waves propagating towards (positive Doppler shift) and away from the radar station (negative Doppler shift). The Doppler frequencies are determined by the phase velocities of the resonant surface gravity waves, superposed on the surface current. In Fig. 2, the vertical dashed lines show the positions of the peaks for the phase velocities on their own. The offset marked df on the diagram is due to the surface current component in the radial direction from the radar station. Taking account of the phase velocity, v_p, for deep-water gravity waves

$$v_p = \sqrt{g/k} \tag{1}$$

we get a Doppler shift f_D given by

$$f_D = \sqrt{\frac{g f_0}{\pi c}} - 2 f_0 \frac{v}{c} \tag{2}$$

where f_0 is the radar frequency, c is the phase speed of electromagnetic waves, and v is the radial component of the surface current. The factor of two is introduced because this is backscatter from a moving target.

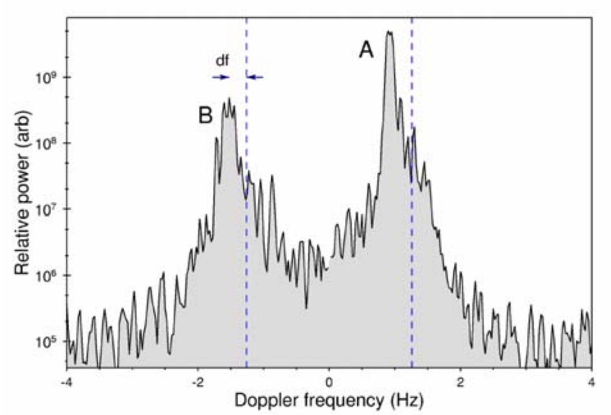

Fig. 2. Typical spectrum for the VHF COSRAD system. The vertical dashed lines mark the theoretical position that the peaks would adopt if there were no surface current. When a surface current is present with a component in the direction of the radial from the radar station, then the peaks move and the offset marked df is a direct measure of that component of the surface current vector.

The VHF COSRAD system is unique in its use of a high frequency in the VHF band. The corresponding Bragg wavelength on the ocean surface is 1 m (for 150MHz), which is at the upper limit of the gravity wave spectrum. At this frequency the Bragg peaks in the Doppler spectrum are broadened and normally there is no clear separation between the first-order and the second-order spectral bands that we see in the HF spectra at 15-30MHz. This line broadening is illustrated in Fig. 2. The second-order theoretical analysis given by Barrick (1972) does not apply in this high VHF band. The energy in the broadened peak is generally more symmetric than in the HF spectra. On one hand, the broadening of the peak tends to detract from the accuracy of locating the centre of the spectral "line". On the other hand, the symmetry tends improve the accuracy of locating the spectral peak. The net result is a small, if any, degradation in the measurement of the radial component of surface current.

Graber et al., (1997) have carried out extensive evaluations of sea surface radar currents against a range of *in situ* measurements. The main variation lies in the fact that the current meter measurements are made at a single point, whereas the radar measurements are averaged over an area of the sea surface.

In the next section we discuss a three-scale basis for considering the effects of swell on the VHF radar spectrum.

3. A THREE-SCALE MODEL FOR SPECTRAL BROADENING

Equation (2) may be considered as a two-scale representation for the Doppler shift spectral line. The Bragg wave ($\lambda_B \approx 1$ m) is at the small scale where the wave-wave interaction involves principles of physical optics, and the effective velocity for the Doppler shift is the phase velocity of the Bragg wave. Surface gravity waves are not purely transverse waves because the disturbed particles undergo a circular perturbation (in deep water) as the wave propagates past a point. We use the term surge velocity to describe the horizontal component of the circular motion, because that is what one experiences when swimming or diving in swell conditions. The surge velocities from waves of long wavelength modulate the Doppler frequency for the backscattered energy from the Bragg waves Conceptually, the surface current may be considered to be the surge current of a wave of very long wavelength ($\lambda \rightarrow \infty$) , and the modulating effect of any other long wave is introduced by its instantaneous velocity. For swell waves where $\lambda_S >> \lambda_B$ we introduce the instantaneous velocity, v_s , provided to the Bragg wave by the swell as

$$v_S = a_S \omega_S \cos(\theta) \cos(\omega_S t) \tag{3}$$

where a_S is the amplitude of the swell wave, ω_S is the angular frequency, and θ is the direction between the swell propagation vector and the radar beam. For a radar on the beach looking out across the surf zone we might reasonably take $\theta = 0$.

The effect of wave breaking is included as a second time-dependent term. The forward bore-like velocity of a breaker is given by the shallow-water wave velocity $\sqrt{Hg}$ where H is the water depth. The breaking event lasts for some fraction of the period of the swell wave, so the instantaneous velocity imposed on the Bragg wave is time dependent. We represent that as a square wave with a short mark/space ratio, m, so the instantaneous velocity due to the breaking front is

$$v_B = \sqrt{Hg}\, M(t) \tag{4}$$

where $M(t)$ takes the value 1 for the fraction m of each swell period.

The velocity terms in equations (3) and (4) produce a frequency modulation on the Bragg echo and this requires us to revert to the time domain. We treat it here by finding a time series for the Bragg wave with its modulation due to the surface current velocity, v, the surge velocity of the swell, and the velocity of the intermittent breaking face. The echo signal is then

$$E(t) = a_B \cos\left\{\omega_B - \frac{2 f_0}{c}\left(v + v_S + v_B\right)\right\} t \tag{5}$$

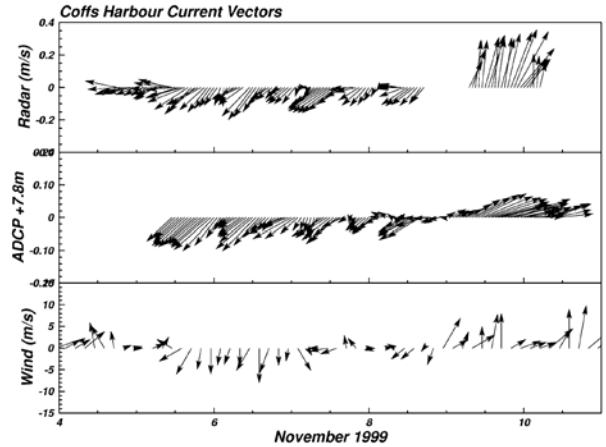

Fig. 3. Flow vectors for the radar pixel in which ADCP1 is located in Fig. 1. The radar data shows surface currents and the ADCP panel shows current vectors at 7.8 m above the bottom. The bottom panel shows wind vectors observed at the Coffs Harbour Airport, about 1 km inland.

We are not evaluating the spectral consequences of equation (5) in this paper, except to point out that we expect frequency modulation of the Bragg peaks to be related to the surge velocities of swell, and long wavelength wind waves at the peak of the wind wave spectrum. The consequence of this modulation clearly is a broadening of the Bragg lines in the spectrum.

4. SYNOPTIC SITUATION

During this short deployment the currents observed on both the ADCP at 7.8 m above the bottom, and the radar at the surface showed five days of southwards flow, followed by about one day of higher speed flow towards the north. These results are shown in Fig. 3 where the bottom panel displays the wind vectors observed at the Coffs Harbour Airport. The water flow in this region is normally southwards driven by the geostrophic western boundary current, which here is known as the East Australian Current. The occasional change to strong winds from the south is known locally as the ‘southerly buster’ which drives the near-shore current northwards for a period of typically one or two days. The southerly buster is caused by a low pressure system crossing the region, followed closely by a high which compressed the isobars. During these conditions Coffs Harbour normally experiences strong winds and swell waves generated in the Tasman Sea.

5. RADAR SPECTRA

The first pixel (up to 100 m from the radar site) always covers white water because, even in calm conditions, the waves break on the beach. Under calm conditions the first-order spectra show broadening for the first three pixels (0 to 300 m range), after which the broadening is significantly less and decreases slowly out to the 15th pixel at a range of 1.5 km.

In rough conditions pixel 3 is in the breaker zone (200 – 300 m) and pixel 15 (1400 – 1500 m) is in the white-cap zone beyond the breakers. Here the overall description is similar; the line broadening decreases quickly over the first 4 pixels, and then decreases more gradually as the range increases.

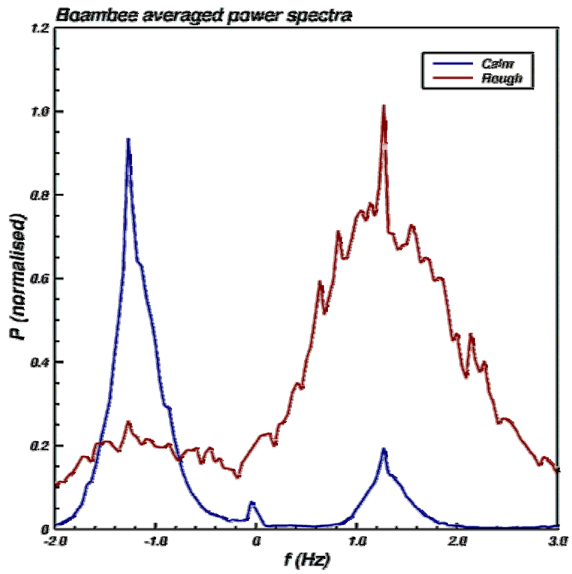

Fig. 4. Average spectrum for the Boambee Beach station under calm conditions (narrow peaks) and rough conditions (broad peaks).

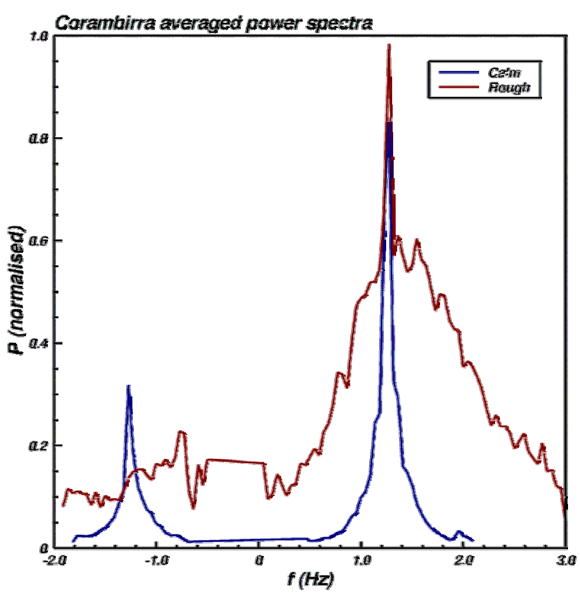

Fig. 5. Average spectrum for the Corambirra Point station under calm conditions (narrow peaks) and rough conditions (broad peaks).

The major difference between calm and rough conditions is shown in Fig. 4 and Fig. 5. These are typical spectra and illustrate the change in broadening of the first-order spectral peak between calm and rough conditions where the magnitude of the line broadening is increased by an order of magnitude.

6. SURFACE CURRENTS

We carried out a self-consistency check on the ADCP data. Each current measurement is the average from 480 pings over a period of 60 s. The standard deviation of the 480 data points was taken as a quality measure of the mean current for each height interval in the water column. The standard deviations are plotted against height above the sea floor in Fig. 7. The standard deviations are uniformly low over the first four height bins (from the bottom) but increase dramatically in bin number 5. This increase is normal for an ADCP and indicates that the surface waves are affecting the current values in that height bin and above. In the comparison with VHF radar surface currents we use the bin centred on 7.8 m.

The scatter plot for radar surface current speed and ADCP current at 7.8 m above the bottom is shown in Fig. 6. The regression line has a slope of 1.84 with a

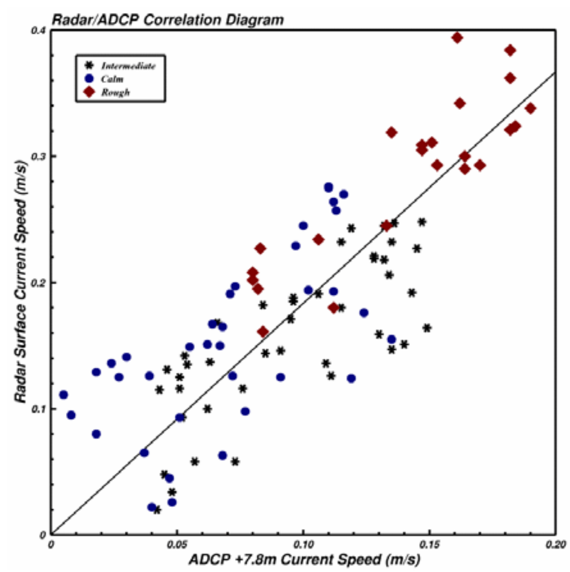

Fig. 6. The correlation plot between VHF radar surface currents and the ADCP 7.8 m currents. The data points are coded for rough, calm and neutral conditions.

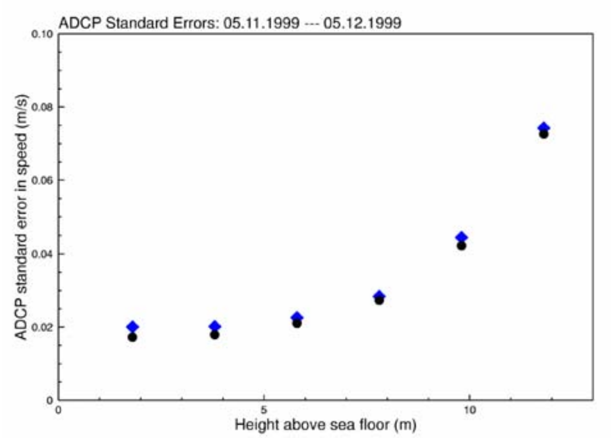

Fig. 7. Standard deviations for the ADCP current measurements. There is a marked increase above about 7.8m.

correlation of 0.82. At the ADCP bin centred on 5.8 m the corresponding slope is 2.17 with a correlation of 0.82. This is an indication of the correlation between the currents in the water column below the wave zone and the surface currents.

In this section we have shown that the first-order Bragg lines in the radar spectra are broadened in the surf zone. Figs 4 and 5 also show that there appears to be sufficient sharpness of the first-order peaks to be able to locate them on the frequency axis. According to (2) it is the frequency of the peak that gives us the surface current component for that station. In terms of (5) which indicates Frequency Modulation, the carrier remains strong as long as the modulation is weak. Heron (2002) discusses how the effective modulation index increases as the radar frequency increases, so that at microwave frequencies the spectra do not have identifiable first-order peaks and the spectral energy is smeared into a broad continuum. In the observations of the surface current in the Coffs Harbour deployment the first-order peaks were generally sufficiently clear to be able to evaluate the surface current.

In Fig. 6 the data points are coded according to whether the conditions were calm, rough, or in between. In general, the calm conditions correspond to data points at the lower currents, and the rough conditions correspond to data points at the higher currents. One observation to be made from Fig. 6 is that the spread of VHF radar points (on the y-axis) is not significantly different under these two sets of conditions.

This indicates that the method for determining the surface currents from the radar spectra is not influenced by the spectral broadening any more than the ADCP at 7.8m.

One other way to check on the effects of rough and breaking waves is to look for discontinuities and features in the 2D surface current maps at the locations where wave breaking occurs.

7. VHF COSRAD SURFACE CURRENT MAPS

By evaluating the component of surface current towards each of the two stations at a point on the sea surface, we can produce the surface current vector. We routinely produced surface current maps for each hour of operation of the system. One such map is shown in Fig. 8 for calm conditions. The main feature of interest was the re-circulation on the leeward side of Corambirra Point. A separation in the flow occurs at the point and comes in to the beach a little to the north of the Boambee Beach radar station. The return flow northwards along the beach is predominantly a wave-driven current. There are no discontinuities or suspicious effects close to the beach in the surf zone.

Fig. 9 shows a typical surface current map under rough conditions. In this case the breaker line is 300-400 m from the beach and there are white caps in the sea beyond that. If there were an adverse effect on the analysis caused by modulation due to breakers, we would expect to see linear effects in the 2D map parallel to the shore.

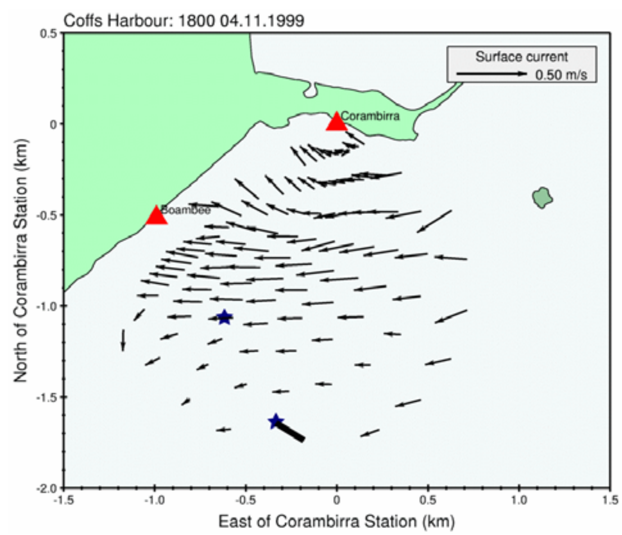

Fig. 8. A typical surface current map for calm conditions. The reference for the scales is the Corambirra radar station.

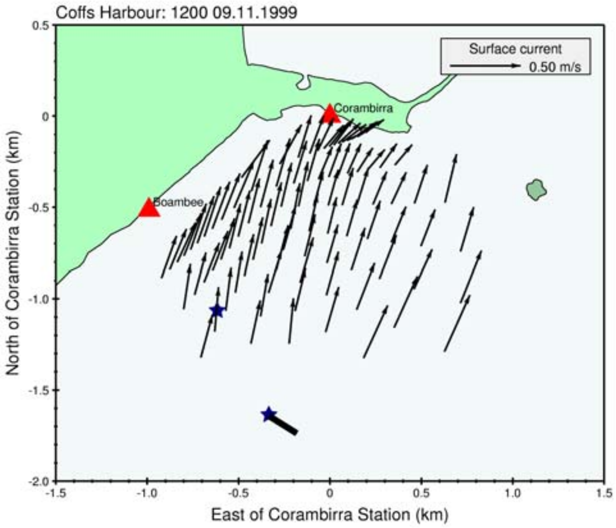

Fig. 9. A typical surface current map for rough conditions. The reference origin for the axes is the Corambirra radar station.

8. CONCLUSIONS

The modulation of the frequency of the Bragg echo by the swell waves underlying the relatively short Bragg waves may be modelled by a three-scale wave structure. The effect is then a frequency modulation, and for low modulation index the carrier (ie the Bragg line) is clear in the spectrum. At higher radar frequencies and/or higher swell amplitudes, the modulation index increases and there comes a point where it is not possible to locate the first-order peaks. This happens for microwave backscatter from the sea where there is a broad band of backscattered energy in the spectrum (Heron, 2002). For the VHF radar operating at 152.2 MHz the technique of determining the surface currents by locating first-order spectral peaks is shown to be valid.

The first order peaks are broadened by the presence of swell and surf. In Fig. 6 the spread of data points is not significantly different between calm and rough conditions. This indicates that the surface current measurements by the radar and the mid-column current measurements by the ADCP have about the same spread under calm and rough conditions. As a separate, but more qualitative evaluation we see no features in the surface current maps which align with the shallow bathymetry that determines the surf breaker line.

It is clear that the first-order lines produced by the VHF radar system operating at frequencies as high as 152.2 MHz are affected by swell waves. We have shown that the location of the peaks is not significantly prejudiced by the effects of swell. The VHF radar technology has potential to monitor rip currents and other horizontal shears in the flow field in the surf zone.

9. ACKNOWLEDGEMENTS

This paper is based on a report to the Coffs Harbour City Council. We appreciate the assistance given by the staff of the Council.

10. REFERENCES

Barrick, D.E., 1972, Remote sensing of sea state by radar, in *Remote Sensing of the Troposphere,* V.E.Derr (Ed), Ch 12, US Govt Printing Office, Washington DC.

Crombie, D.D., 1955, Doppler spectrum of sea echo at 13.56 Mc/s, Nature, **175**, 681-682.

Graber, H.C., B.K. Haus, R.D. Chapman and L.K. Shay, 1997, HF radar comparisions with moored estimates of current speed and direction: Expected differences and implications, J.Geophys.Res., **102(C8)**, 18749-18766.

Heron, M.L., 2002, Applying a unified directional wave directional wave spectrum to the remote sensing of wind-wave directional spreading, Canadian J. Remote Sensing, **28**, 346-353.

Prytz, A. and M.L. Heron, 2000, Report on Ocean Currents off Boambee Beach, for Coffs Harbour City Council, Feb. 2000.